TOWARD GEOMETRIC CONTROL OF LATE-STAGE DIFFUSION PROPERTIES FOR 3D PRINTED BIODEGRADABLE MICROSTRUCTURES

Emmett Z. Freeman†, Eleanor C. Grosvenor†, Ian B. Rosenthal†, Ruben Acevedo, and Ryan D. Sochol
Department of Mechanical Engineering, University of Maryland, College Park, Maryland, USA
† These authors contributed equally to the work (listed alphabetically)

ABSTRACT

The ability to manufacture biodegradable structures at small scales is integral to a variety of applications in biological, medical, and pharmaceutical fields. Recent developments in additive manufacturing (or "three-dimensional (3D) printing") allow for biodegradable materials to be printed with high resolution; however, there is typically a limit with respect to a resolvable feature size (*e.g.*, layer height) that dictates the minimum increments for tuning distinct degradation-mediated functionalities *via* print geometry. Here we investigate the potential to 3D print designs that afford additional degrees of control during intermediate stages between the complete biodegradation of microstructures that differ by a single layer height. Preliminary fabrication results revealed effective printing of tubular 3D biodegradable gelatin methacryloyl (GelMA) structures with outer diameters of 100 μm and wall thicknesses of 35 μm using two-photon direct laser writing (DLW)-based additive manufacturing. Simulation results for varying designs suggest that both the total degradation time as well as the diffusion dynamics through a microstructure during the final stage of biodegradation can be modulated *via* geometric means. Thus, the concepts presented in this work could open new avenues in areas including drug delivery and biomaterials.

KEYWORDS

Biodegradation, Additive Manufacturing, 3D Printing, Direct Laser Writing, Two-Photon Polymerization

INTRODUCTION

Biodegradable materials underlie a wide array of applications across fields including controlled-release drug delivery, wound healing, and biological research [1]. Although researchers have developed numerous methods to engineer biodegradable particles, structures, and systems [2], the predominant reliance on traditional micro- and nanofabrication protocols that lack flexibility in geometric design customization has impeded progress and technology utility [3,4]. Consequently, there is growing interest in alternatives in the form of additive manufacturing (also referred to as "3D printing") [5].

In recent years, researchers have applied diverse additive manufacturing approaches to construct microsystems [6,4]. For applications associated with biodegradable materials, the breadth of material selection is an important metric for evaluating a technology [7]. Unfortunately, commercial inkjet-based additive manufacturing techniques offer extremely limited choices in printable materials [8,9]. Conversely, nozzle-based 3D printing techniques, such as direct ink writing (DIW), are compatible with a vast assortment of extrudable materials [10]. Despite this benefit, however, such printing methods suffer from long print time requirements as the nozzle must physically move from point to point to deposit material [11]. This problem is exacerbated when printing structures at smaller length scales [12]. Thus, to simultaneously balance material selection, print speed, and feature resolution, researchers have turned to photopolymerization-based additive manufacturing methods [13,14], such as stereolithography (SLA), digital light processing (DLP) printing, and direct laser writing (DLW) [15-17]. Among these technologies, DLW provides the highest resolutions for feature definition, typically on the order of hundreds of nanometers [18,19].

In prior work, the Metin Sitti group demonstrated the ability to print biodegradable gelatin methacryloyl (GelMA) microswimmers with lengths of 20 μm and diameters of 6 μm using DLW [20]. Meanwhile, other groups have reported DLW-printed structures that, if further combined with emerging biodegradable materials, could provide a powerful pathway to advancing biomedical applications [21,22]. One caveat, however, is that additive manufacturing strategies are often limited by defined parameters, such as the minimum layer height [23]. When printing a biodegradable material, such parameters inherently set increments in performance, particularly in the final stage of biodegradation. Thus, in this work, we seek to elucidate the design space for expanding the functionality of 3D printed biodegradable microstructures.

CONCEPT

As an exemplar, we consider the case of a microstructure that contains a liquid core that is intended to be released at a particular time (**Fig. 1a**). Using DLW, a biodegradable "capping" microstructure is printed by scanning a pulsed IR laser in a point-by-point, layer-by-layer fashion (**Fig. 1b**). Notably, the entirety of the cap is designed to be solid with the exception of the final top layer, which includes a custom geometric design (**Fig. 1c**). In a situation that promotes biodegradation, the cap degrades leading up to the penultimate stage in which only the geometric design remains (**Fig. 1d**). As a result, the core is able to diffuse out of the container, but with the diffusion behavior modified based on the residual geometry (**Fig. 1d**).

To evaluate the capability of this potential, we considered six cap designs. We included two control caps that differed in thickness by one layer height. For the purposes of this study, the thinner cap included a thickness, T_O, of 1.0 μm (**Fig. 1e**), and the thicker cap included a thickness, T_I, of 1.1 μm (**Fig. 1f**), corresponding to the minimum layer height of 100 nm associated with the Nanoscribe Photonic Professional GT2 DLW 3D printer (Nanoscribe GmbH, Karlsruhe, Germany). We also designed two crosshatch patterns (**Fig. 1g,h**) and a concentric arrangement (**Fig. 1i**)—all corresponding to

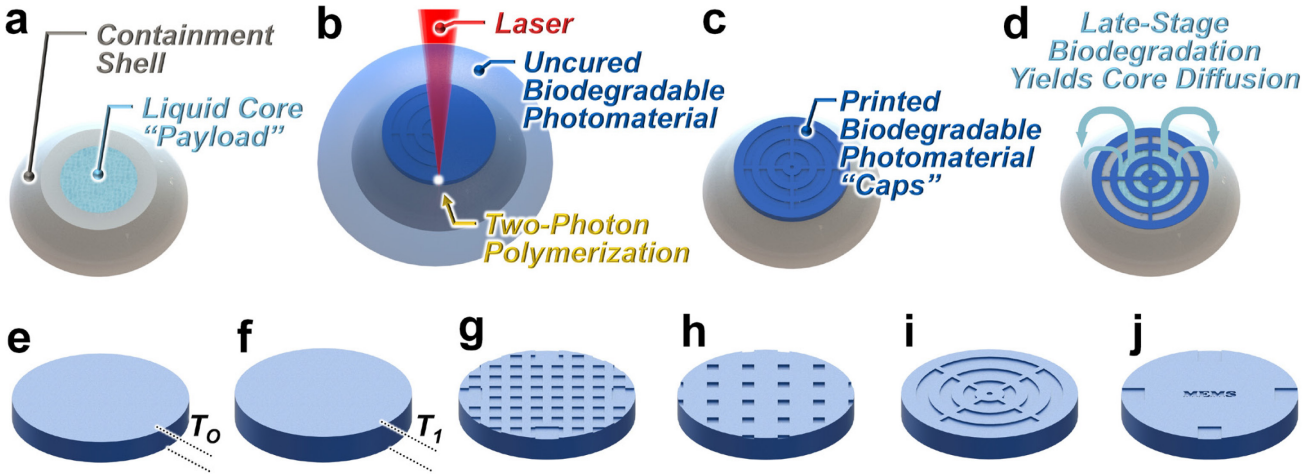

Figure 1: Conceptual illustrations of the direct laser writing (DLW) process to print biodegradable caps with geometric designs that influence diffusion properties during the final stage of biodegradation. *(**a**) Initially, a liquid payload is localized within a containing structure. (**b**) A pulsed IR laser is scanned to cure a biodegradable photomaterial through two-photon polymerization. (**c**) The surface of the printed biodegradable cap includes a geometric design that is the thickness of one layer height. (**d**) In the final stage of biodegradation, only the custom geometric design remains, which alters the diffusion behavior associated with the core payload. (**e-j**) Distinct geometric designs for the caps: (**e**) T_0 control, (**f**) T_1 control, (**g**) small crosshatches, (**h**) large crosshatches, (**i**) concentric, and (**j**) "MEMS". The thickness, T_1, is one 3D printing layer height larger than T_0.*

distinct surface areas. Lastly, we included one "MEMS" design in which the word "MEMS" was the only part embossed in the final layer (**Fig. 1j**).

MATERIALS AND METHODS

DLW-Printing of GelMA Structures

The computer-aided design (CAD) software, SolidWorks (Dassault Systèmes, France), was used to generate a 3D model of cylindrical microtube structure. The model was exported as an STL file and then imported into the computer-aided manufacturing (CAM) software, DeScribe (Nanoscribe), for printing with the Nanoscribe Photonic Professional GT2 DLW system. A droplet of a solution consisting of 87% DI water, 10% GelMA (Sigma-Aldrich), and 3% lithium phenyl(2,4,6 trimethylbenzoyl) phosphinate (LAP) was used as the photocurable material for DLW printing (**Fig. 2a**). GelMA structures were printed in the oil-immersion configuration with a laser power of 40 mW and a laser scanning speed of 3,000 μm/s. The GelMA structures were then removed from the printer and developed (**Fig. 2b**). Scanning electron microscope (SEM) images of fabrication results were captured using a TM4000 Tabletop SEM (Hitachi, Tokyo, Japan).

Theoretical Simulations

SolidWorks (Dassault Systèmes) was used to generate 3D models of all of the cap designs. The material properties feature was used to analyze complex geometries and determine the volume of each structure for computation *via* an analytic degradation model:

$$V(t) = V_0 - \lambda t \qquad (1)$$

where $V(t)$ is the volume at a given time, V_0 is the initial volume, λ is the decay constant, and t is time. GelMA biodegradation rates were using previously reported data presented by Yoon *et al.* [24].

For simulations of diffusion phenomena associated with late-stage cap degradation geometries, a tube with an outer diameter of 15.5 μm was extruded from the midplane of the geometry without merging using SolidWorks in order to provide a geometry through which the fluid can flow. Each model was exported as a .STEP file, and then imported to the finite element analysis (FEA) software, COMSOL Multiphysics 5.2 (COMSOL Inc., Sweden). Water was used to model the liquid core. A laminar flow study was run to determine the fluidic velocity and pressure as the water exited the cap. These values were transferred

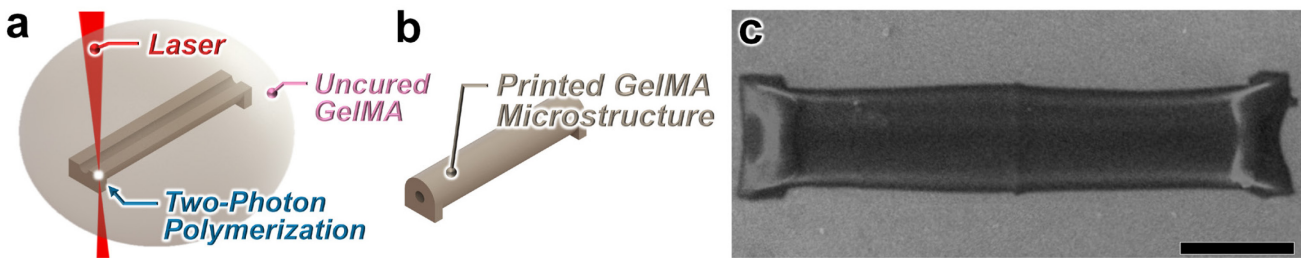

Figure 2: Conceptual illustrations and SEM results for the use of DLW to print biodegradable gelatin methacryloyl (GelMA) structures. *(**a**) A pulsed IR laser is scanned to cure a photocurable GelMA material through two-photon polymerization. (**b**) After development, a printed GelMA structure remains. (**c**) SEM micrograph of a hollow GelMA tube. Scale bar = 100 μm.*

to a particle trace for fluid flow study to compute the paths taken by particles within the fluid. Each particle was assigned a diameter of 10 nm and a density of 2.2×10^3 kg/m^3. A Poincaré map plotted the positions of the released particles and rendered those images to model the path.

RESULTS AND DISCUSSION

DLW Fabrication of GelMA Microstructures

To provide a preliminary investigation into the capabilities associated with printing biodegradable GelMA microstructures using DLW-based additive manufacturing, we designed and fabricated hollow tubular components. The printing results revealed effective fabrication of hollow GelMA tubes with an outer diameter of 100 μm, a length of 500 µm, and a wall thickness of 35 µm (**Fig. 2c**). It is important to note that we found print efficacy to rely heavily on the printing parameters, with lower laser powers and/or higher scan speeds resulting in print failures based on unsuccessful curing. Nonetheless, the presented results demonstrate that such parameters can be tuned to yield successful GelMA prints, which is consistent with prior works from other groups [20].

Biodegradation Analysis

The total time required for each cap design to degrade serves as a benchmark for basic component functionality. The biodegradation behavior for the caps were initially modeled analytically using **Equation 1**. As a means to compare the degradation rates among the varying designs, we quantified a "Relative Biodegradation Time (*RBT*)" performance metric as:

$$RBT = \frac{t - t_{min}}{t_{max} - t_{min}} \quad (2)$$

where t is the degradation time for a particular design, and t_{min} and t_{max} are the degradation times of the T_O and T_1 control caps, respectively. The quantified *RBT* results revealed that the distinct designs are able to effect differences in the biodegradation performance (**Fig. 3**).

Nanoparticle Diffusion Analysis

To investigate the diffusion characteristics associated with late-stage biodegradation of the caps—*i.e.*, at which point only the geometric designs remain—we modeled the transmission probabilities of 10-nm particles through each cap (**Fig. 4a–e**). For quantification of these diffusion-associated behaviors, we calculated a "Relative Diffusion Rate (*RDR*)" performance metric as:

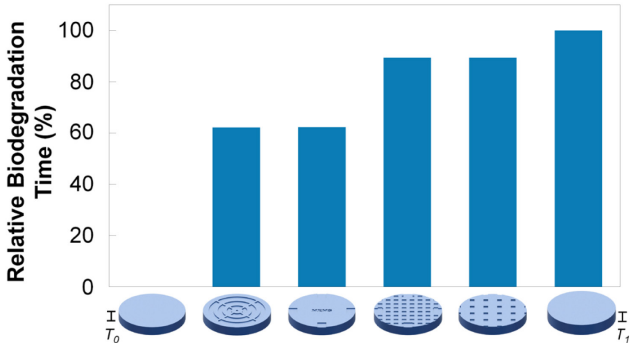

Figure 3: Quantified results for Relative Biodegradation Time (RBT) versus varying 3D printed cap geometries. *T_O = 1 µm; T_1 = 1.1 µm; RBT values quantified via* ***Eq. 2****.*

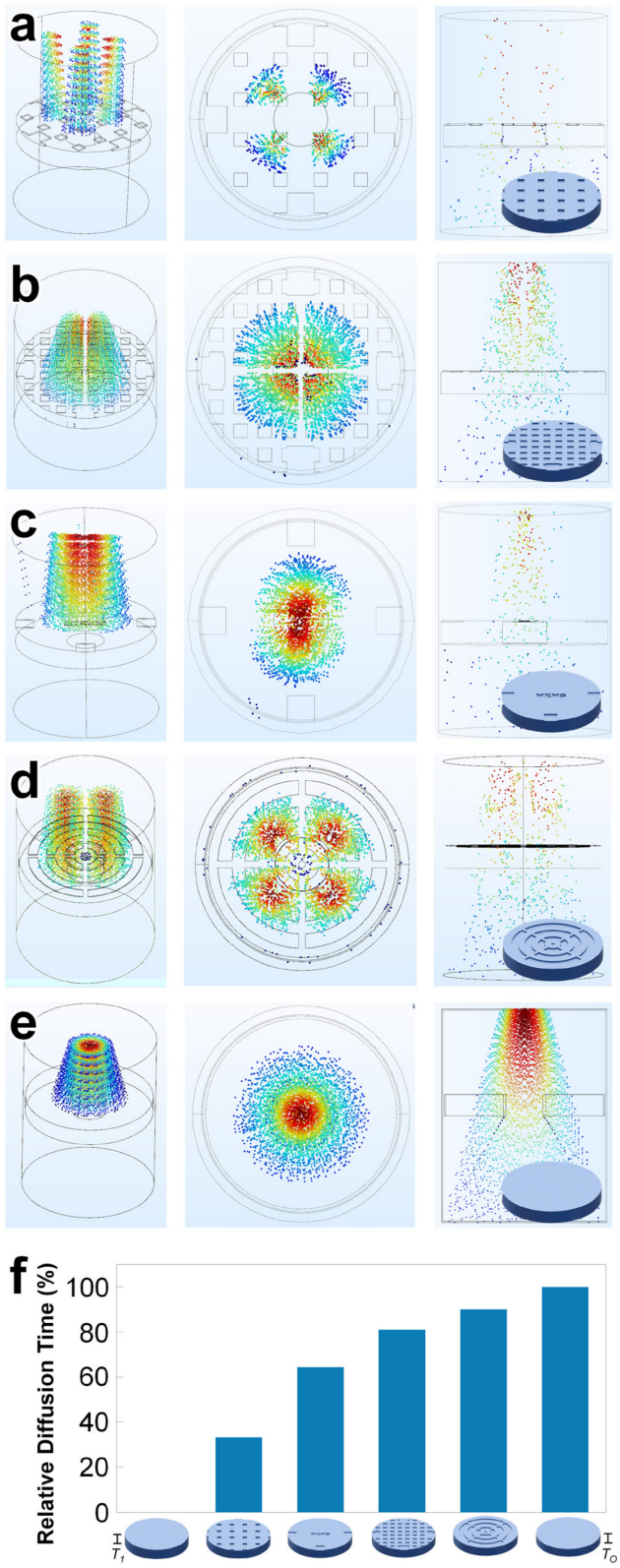

Figure 4: COMSOL simulation results for diffusion characteristics associated with varying cap geometries during late-stage biodegradation. *(**a–e**) Nanoparticle diffusion behaviors associated with distinct cap designs. (**f**) Relative Diffusion Rate (RDR) versus cap geometry. T_O = 1 µm; T_1 = 1.1 µm; RBT values quantified via* ***Eq. 3****.*

$$RDR = \frac{p - p_{min}}{p_{max} - p_{min}} \quad (3)$$

where p is the transmission probability for a particular design, and p_{max} and p_{min} are the transmission probabilities for the T_O and T_I control caps, respectively. The quantified *RDR* results revealed gradual intermediate variations in diffusion characteristics enabled by geometric designs the thickness of a single 3D printing layer height (**Fig. 4f**).

CONCLUSIONS

In this study, we investigated the ability to use additive manufacturing-enabled geometric designs to modulate liquid core release behaviors associated with late-stage biodegradation of 3D printed sealing microstructures. The preliminary results suggest that the presented concept holds promise for tuning biodegradation-mediated biochemical release functionalities; however, future work is needed to experimentally validate these capabilities. Nonetheless, this strategy offers a pathway to new applications in biomedical and pharmaceutical domains.

ACKNOWLEDGEMENTS

We greatly appreciate the contributions of Michael Restaino, Abdullah T. Alsharhan, and the members of the Bioinspired Advanced Manufacturing (BAM) Laboratory and Terrapin Works at the University of Maryland. This work was supported in part by US NSF Award 1943356.

REFERENCES

[1] M. Mahmoudi *et al.*, "Multiscale technologies for treatment of ischemic cardiomyopathy," *Nat. Nanotech.,* vol. 12, no. 9, pp. 845–855, 2017.

[2] S. Roberts *et al.*, "Complex microparticle architectures from stimuli-responsive intrinsically disordered proteins," *Nat. Comm.*, vol. 11, no. 1, pp. 1–10, 2020.

[3] A. C. Daly, L. Riley, T. Segura, and J. A. Burdick, "Hydrogel microparticles for biomedical applications," *Nat. Rev. Mat.*, vol. 5, no. 1, pp. 20–43, 2020.

[4] G. Weisgrab, A. Ovsianikov, and P. F. Costa, "Functional 3D Printing for Microfluidic Chips," *Adv. Mater. Technol.*, vol. 4, no. 10, p. 1900275, 2019.

[5] S. K. Saha and S. Chen, "Comment on 'Rapid Assembly of Small Materials Building Blocks (Voxels) into Large Functional 3D Metamaterials,'" *Adv. Funct. Mater.*, vol. 30, no. 30, p. 2001060, 2020.

[6] E. H. Childs, A. V. Latchman, A. C. Lamont, J. D. Hubbard, and R. D. Sochol, "Additive Assembly for PolyJet-Based Multi-Material 3D Printed Microfluidics," *J. Microelectromech. Syst.*, vol. 29, no. 5, pp. 1094–1096, 2020.

[7] R. S. Riley, C. H. June, R. Langer, and M. J. Mitchell, "Delivery technologies for cancer immunotherapy," *Nature Reviews Drug Discovery*, vol. 18, no. 3, pp. 175–196, 2019.

[8] R. Sochol *et al.*, "3D printed microfluidic circuitry via multijet-based additive manufacturing," *Lab on a Chip*, vol. 16, no. 4, pp. 668-678, 2016.

[9] E. Sweet, R. Mehta, Y. Xu, R. Jew, R. Lin, and L. Lin, "Finger-powered fluidic actuation and mixing *via* MultiJet 3D printing," *Lab on a Chip*, vol. 20, no. 18, pp. 3375–3385, 2020.

[10] J. Norman *et al*, "A new chapter in pharmaceutical manufacturing: 3D-printed drug products," *Advanced Drug Delivery Reviews*, vol. 108, pp. 39–50, 2017.

[11] R. Su *et al.*, "3D printed self-supporting elastomeric structures for multifunctional microfluidics," *Sci. Adv.*, vol. 6, no. 41, p. eabc9846, 2020.

[12] A. Naderi, N. Bhattacharjee, and A. Folch, "Digital Manufacturing for Microfluidics," *Annu. Rev. Biomed. Eng.*, vol. 21, no. 1, pp. 325–364, 2019.

[13] S. Tasoglu *et al*, "Untethered micro-robotic coding of three-dimensional material composition," *Nat Commun.*, vol. 5, no. 1, p. 3124, 2014.

[14] T. Ching, Y.-C. Toh, and M. Hashimoto, "Fabrication of Complex 3D Fluidic Networks via Modularized Stereolithography," *Adv. Eng. Mater.*, vol. 22, no. 3, p. 2070012, 2020.

[15] A. P. Kuo, N. Bhattacharjee, Y. Lee, K. Castro, Y. T. Kim, and A. Folch, "High-Precision Stereolithography of Biomicrofluidic Devices," *Adv. Mater. Technol.*, vol. 4, no. 6, p. 1800395, 2019.

[16] H. Gong, B. P. Bickham, A. T. Woolley, and G. P. Nordin, "Custom 3D printer and resin for 18 μm × 20 μm microfluidic flow channels," *Lab Chip*, vol. 17, no. 17, pp. 2899–2909, 2017.

[17] A. C. Lamont, M. A. Restaino, M. J. Kim, and R. D. Sochol, "A facile multi-material direct laser writing strategy," *Lab Chip*, vol. 19, no. 14, pp. 2340–2345, 2019.

[18] A. T. Alsharhan, R. Acevedo, R. Warren, and R. D. Sochol, "3D microfluidics *via* cyclic olefin polymer-based *in situ* direct laser writing," *Lab Chip*, vol. 19, no. 17, pp. 2799–2810, 2019.

[19] A. C. Lamont, A. T. Alsharhan, and R. D. Sochol, "Geometric Determinants of In-Situ Direct Laser Writing," *Sci Rep*, vol. 9, no. 1, p. 394, 2019.

[20] H. Ceylan, I. C. Yasa, O. Yasa, A. F. Tabak, J. Giltinan, and M. Sitti, "3D-Printed Biodegradable Microswimmer for Theranostic Cargo Delivery and Release," *ACS Nano*, vol. 13, no. 3, pp. 3353–3362, 2019.

[21] Y. C. Saraswat, F. Ibis, L. Rossi, L. Sasso, H. B. Eral, and P. Fanzio, "Shape anisotropic colloidal particle fabrication using 2-photon polymerization," *Journal of Colloid and Interface Science*, vol. 564, pp. 43–51, 2020.

[22] R. Acevedo, M. A. Restaino, D. Yu, S. W. Hoag, S. Flank, and R. D. Sochol, "3D Nanoprinted Liquid-Core-Shell Microparticles," *J. Microelectromech. Syst.*, vol. 29, no. 5, pp. 924–929, Oct. 2020.

[23] A. T. Alsharhan, A. J. Stair, R. Acevedo, T. Razaulla, R. Warren, and R. D. Sochol, "Direct Laser Writing for Deterministic Lateral Displacement of Submicron Particles," *J. Microelectromech. Syst.*, vol. 29, no. 5, pp. 906–911, 2020.

[24] H. J. Yoon *et al.*, "Cold Water Fish Gelatin Methacryloyl Hydrogel for Tissue Engineering Application," *PLoS ONE*, vol. 11, no. 10, 2016.

CONTACT

*R.D. Sochol, tel: +1 (301) 405-6928; rsochol@umd.edu